Quantum phase transition in the U(4) vibron model and the E(3) symmetry

Yu Zhang (张宇),[1] Zhan-feng Hou (侯占峰),[1] Huan Chen (陈欢),[1] Haiqing Wei (尉海清),[2] and Yu-xin Liu (刘玉鑫)[1,3,*]

[1]*Department of Physics and State Key Laboratory of Nuclear Physics and Technology, Peking University, Beijing 100871, China*

[2]*School of Information Science and Engineering, Lanzhou University, Lanzhou 730000, China*

[3]*Center of Theoretical Nuclear Physics, National Laboratory of Heavy Ion Accelerator, Lanzhou 730000, China*

(Received 26 November 2007; revised manuscript received 8 July 2008; published 25 August 2008)

We study the details of the U(3)–O(4) quantum phase transition in the U(4) vibron model. Both asymptotic analysis in the classical limit and rigorous calculations for finite boson number systems indicate that a second-order phase transition is still there even for the systems with boson number N ranging from tens to hundreds. Two kinds of effective order parameters, including $E1$ transition ratios $B(E1:2_1 \to 1_1)/B(E1:1_1 \to 0_1)$ and $B(E1:0_2 \to 1_1)/B(E1:1_1 \to 0_1)$, and the energy ratios E_{2_1}/E_{0_2} and E_{3_1}/E_{0_2} are proposed to identify the second-order phase transition in experiments. We also found that the critical point of phase transition can be approximately described by the E(3) symmetry, which persists even for moderate $N \sim 10$ protected by the scaling behaviors of quantities at the critical point. In addition, a possible empirical example exhibiting roughly the E(3) symmetry is discussed.

DOI: 10.1103/PhysRevC.78.024314 PACS number(s): 21.60.Fw, 05.70.Fh, 21.10.Re, 21.60.Ev

I. INTRODUCTION

Recently, quantum phase transitions in mesoscopic systems (systems with a finite number of particles N), such as atomic nuclei [1–19], molecules [20–22], atomic clusters [23], and finite polymers, have been attracting a lot of interest. The transitions in these systems are between different shapes, geometric configurations, or modes of collective motions. It is of great interest to study the characteristics of the phase transitions subject to the finiteness of these systems [7]. Algebraic approaches provide a convenient way to investigate the phase transitions in mesoscopic systems. The best example may be the interacting bosons model (IBM) [5], which has been widely implemented to study shape phase transitions in nuclei.

Many features of the phase transitions and their orders in nuclei have been well identified in the IBM (see, for example, Refs. [1,7,11,12,16,17]). Another important algebraic model is the U(4) vibron model [20,24], which has been mainly used to characterize the relative motion of a dipole-deformation in the three-dimensional space, so to provide an algebraic framework to describe the behavior of rotational and vibrational motions of two-body (or two-cluster) systems such as diatomic molecules [24–26], binary clusters [27–30], $q\bar{q}$ mesons [31,32], and so on. It has been shown that the U(4) model involves two dynamical symmetries, namely U(3) and O(4). Soon after the model was developed, the phase transition from U(3) to O(4) symmetry was identified to be of second order [33]. Nevertheless, there were contradictory predictions that the phase transition was of first order [23]. In IBM, the shape transition still persists even for the boson number $N \sim 10$ [7,11,12,16,17], which corresponds to the typical number of pairs of the valence nucleons. The typical number of bosons used to describe experiments in the vibron model ranges also from tens to hundreds. Even though a general approach has been developed for two level systems [7,11,12], detailed investigations on the phase transition in the vibron model, especially the dependence on the boson number and the critical behavior are still lack. Additionally, a new class of symmetries, so-called representation symmetries [34,35], was introduced by Iachello to describe the properties of nuclei at the critical point of phase transitions in IBM and greatly confirmed in experiments (see, for example, Refs. [36,37]), although seen later in this article, this kind of symmetry can also be found to work well at the critical point of the phase transition in vibron model. We will then discuss the related issues in this article.

The article is organized as follows. In Sec. II, we describe briefly the U(4) vibron model and analyze the phase transition in the model in large boson number limit. In Sec. III, we analyze the phase transition in the case of finite boson number and discuss the effect of the finiteness of boson number. In Sec. IV, we discuss a possible empirical example of the system in the E(3) symmetry. Finally in Sec. V, we give a summary and some remarks.

II. PHASE TRANSITION IN U(4) VIBRON MODEL IN LARGE N LIMIT

In the U(4) model, elementary excitations are dipole p bosons with spin and parity $J^\pi = 1^-$ and scalar s-bosons with $J^\pi = 0^+$. Given the total number of bosons and the angular momentum being conserved, there are only two dynamic symmetry limits, U(3) and O(4). Accordingly, there exist two dynamic symmetry chains:

$$U(4) \supset U(3) \supset O(3), \quad \text{(I)} \tag{1}$$

$$U(4) \supset O(4) \supset O(3). \quad \text{(II)} \tag{2}$$

It has been shown that the U(3) symmetry corresponds to nonrigid ro-vibrations, whereas the O(4) symmetry represents rigid ro-vibrations [24]. A general Hamiltonian of the U(4)

*yxliu@pku.edu.cn

vibron model with only one- and two-body interactions can be expressed in terms of linear and quadratic invariant operators (Casimir operators) of all the subgroups contained in the dynamic group chains.

To study the characteristic of the phase transition from the U(3) symmetry to the O(4) symmetry in the U(4) vibron model, one starts usually with the Hamiltonian

$$\hat{H} = \varepsilon[(1-\eta)\hat{n}_p - \frac{\eta}{f(N)}\hat{D}\cdot\hat{D}], \tag{3}$$

where ε is a scale parameter and may be set to 1 for convenience without loss of generality, $\hat{n}_p = \sum_m p_m^\dagger p_m$ is the number operator of p bosons, $\hat{D}_q^{(1)} = (s^\dagger \tilde{p} + p^\dagger s)_q^{(1)}$ is the electric dipole operator with $\tilde{s} = s$ and $\tilde{p}_m = (-1)^{-m} p_{-m}$, $f(N)$ is a linear function of total number of bosons N, and η is a control parameter for this model. It is straightforward to show that such a Hamiltonian can be rewritten as

$$\hat{H} = \varepsilon(1-\eta)C_{1U(3)} - \varepsilon\frac{\eta}{f(N)}C_{2O(4)} + \varepsilon\frac{\eta}{f(N)}C_{2O(3)}. \tag{4}$$

It is apparent that the system is in the U(3) symmetry when $\eta = 0$ and changed into the O(4) symmetry when $\eta = 1$. By varying $\eta \in [0, 1]$, one can realize a U(3)–O(4) phase transition.

We can investigate the geometric configuration of the model in the framework of intrinsic coherent state approach (see, for example, Ref. [20]; a method beyond the mean field can be found in Refs. [11,12]). The classical limit corresponding to the Hamiltonian in Eq. (3) is obtained by considering its expectation value in the coherent state [20]

$$|N;\mathbf{t}\rangle = (N!)^{-1/2}[(1-\mathbf{t}^*\cdot\mathbf{t})^{1/2}s^\dagger + \mathbf{t}\cdot\mathbf{p}^\dagger]^N|0\rangle, \tag{5}$$

where $\mathbf{t}$ is a complex three-dimensional vector and its complex conjugate is denoted by $\mathbf{t}^*$. The classical Hamiltonian is given by $H_{\rm cl} = \langle N;\mathbf{t}|H|N;\mathbf{t}\rangle$. One may introduce the canonical position and momentum variables $\mathbf{x}$ and $\mathbf{q}$ by the transformation [20]

$$\mathbf{t} = (\mathbf{x} + i\mathbf{q})/\sqrt{2}, \quad \mathbf{t}^* = (\mathbf{x} - i\mathbf{q})/\sqrt{2}. \tag{6}$$

The classical potential is just the value of $H_{\rm cl}(q, x)$ with $q = 0$, where $|\mathbf{x}| = x$ and $|\mathbf{q}| = q$,

$$V(x) = H_{\rm cl}(q = 0, x). \tag{7}$$

When $f(N)$ in Eq. (3) is set to $3N$, the potential in the Hamiltonian can be nicely written as

$$V(x) = N\left[(1-\eta)\frac{x^2}{2} - \frac{\eta}{3}x^2(2-x^2)\right]. \tag{8}$$

It is evident that the classical limit of the U(3) symmetry is a three-dimensional harmonic vibrator with $V_{U(3)}(x) = \frac{N}{2}x^2$ [corresponding to $\eta = 0$ in Eq. (8)]. By contrast, the classical potential becomes $V_{O(4)}(x) = -\frac{N}{3}x^2(2-x^2)$ in the O(4) symmetry (corresponding to $\eta = 1$), which is just the Morse potential commonly used to describe the ro-vibration spectrum of rigid diatomic molecules, after a transformation of variable $x^2 = e^{-\beta(r-r_e)}$ [20], where r is the relative coordinate, r_e is the equilibrium separation, and β is a range parameter.

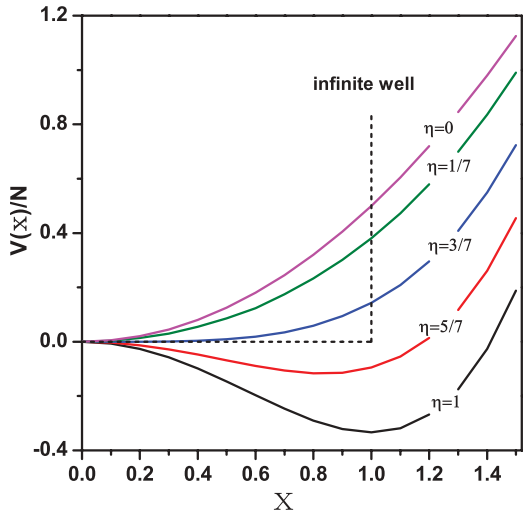

FIG. 1. (Color online) The potential energy surface $\frac{1}{N}V(x,\eta)$ (in the range $x \geqslant 0$) as a function of x with the control parameter $\eta = 0, 1/7, 3/7, 5/7, 1$, respectively, and the infinite well as an approximation of the potential at the critical point $\eta = 3/7$.

The order of the phase transition U(3)–O(4) may be determined with the standard approach (see, for instance, Ref. [5]). By analyzing the stability of the system with the potential of Eq. (8), we find that $V_{\rm min}(x) = 0$ for $\eta < \frac{3}{7}$, and $V_{\rm min}(x) = -\frac{N}{48}\frac{(7\eta-3)^2}{\eta}$ for $\eta > \frac{3}{7}$. It is evident that, at the critical point $\eta_c = \frac{3}{7}$, $\frac{\partial V(x)_{\rm min}}{\partial \eta}$ is continuous, but $\frac{\partial^2 V(x)_{\rm min}}{\partial \eta^2}$ is discontinuous. It indicates apparently that the phase transition from U(3) symmetry to O(4) symmetry is in second order, which is consistent with the result given in Ref. [33] but different from that in Ref. [23].

To understand the phase structure and the phase transition further, we illustrate the classical potential $\frac{1}{N}V(x,\eta)$ at several values of the control parameter η in Fig. 1. Easily seen from the figure, for $\eta < \frac{3}{7}$, the potential energy surface has only one minimum at $x = 0$; for $\eta > \frac{3}{7}$, the potential energy surface reaches minimum at nonzero values of x, more specifically, at $x_e = \pm\sqrt{\frac{7\eta-3}{4\eta}}$. x_e can be taken as the classical order parameter, then one can extract the critical exponent $u = 1/2$ by expanding around the critical point η_c as $[x_e - x_e(\eta_c)] \propto (\eta - \eta_c)^u$ [7]. Furthermore, the potential energy surface becomes rather flat around the critical point $\eta_c = \frac{3}{7}$ (to be more explicit, it takes the form $V_{\rm cri}(x) = \frac{N}{7}x^4$) and is similar to the bottom of infinite well. Such a variational behavior confirms the second-order nature of the U(3)–O(4) phase transition (analogous to that of the E(5) symmetry in the vibration to γ-soft rotation, i.e., the U(5)–O(6) phase transition in the IBM [34]), and the critical value of the control parameter $\eta_c = \frac{3}{7}$ [in general case of $f(N) = aN$ in Eq. (3), we have $\eta_c = \frac{a}{4+a}$]. In addition, it is consistent with the result given in the catastrophe theory [38].

In view of the above characteristic of the potential energy surface at the critical point (with $\eta_c = \frac{3}{7}$), and following Ref. [34], one may approximate the potential around the

TABLE I. Excitation energies of low-lying states in the E(3) symmetry (in arbitrary unit).

	$\xi = 1$	$\xi = 2$	$\xi = 3$
$L = 0$	0	2.87	7.65
$L = 1$	1	4.83	10.57
$L = 2$	2.26	7.06	13.77
$L = 3$	3.77	9.56	17.23

critical point by a three-dimensional infinite well

$$V(x) = \begin{cases} 0, & x \leqslant x_W, \\ \infty, & x > x_W. \end{cases} \tag{9}$$

As is well known, the dynamics in a three-dimensional infinite well can be described with a Bessel equation with solutions involving Bessel functions. One can then denote the symmetry at the critical point in the vibron model as E(3), which differs from that in the IBM (E(5) symmetry in the transition from U(5) to O(6) symmetry [34]) only in the dimension. In E(3) symmetry, all the quantities can be calculated as done in E(5) symmetry. The excitation energy can be determined as $E_{L_\xi} = \frac{2B}{\hbar} k_{\xi,L}^2$ and $k_{\xi,L} = \frac{y_{\xi,L}}{x_W}$, where $y_{\xi,L}$ is the ξth zero of $J_{L+1/2}(z)$ and B is a constant. Then, the eigenfunctions can be written as $\psi(x, \theta, \varphi) = C_{k,L} j_L(kx) Y_{L,M}(\theta, \varphi)$, with $j_L(kx) = \sqrt{\frac{\pi}{2kx}} J_{L+1/2}(kx)$ being the solution of radial equation, the spheric harmonics function $Y_{L,M}(\theta, \varphi)$ is the solution of angular part, and the normalization constants $C_{k,L}$ can be determined by imposing the condition $\int_0^\infty |C_{k,L} j_L(kx)|^2 x^2 dx = 1$.

We give in Table I the excitation energies of some low-lying states in E(3) symmetry, where the energy of ground state is set to zero and all energies are normalized to the energy of the first excited state. Noteworthy from Table I are some typical energies ratios such as E_{2_1}/E_{1_1}, E_{3_1}/E_{1_1} and so on, where the state are denoted by L_ξ. Electromagnetic transition rates can also be calculated by taking matrix elements of the dipole operator $T(E1) = \alpha x Y_{1,M}(\theta, \varphi)$, where α is a scale factor. It should be noted that the symmetry fixes uniquely all transition rates $B(E1, L \to L-1)$ in terms of an overall scale; we are more interested in the $B(E1)$ ratios, some of which are listed in Table II.

III. PHASE TRANSITION IN U(4) VIBRON MODEL IN FINITE N CASE

The analysis above shows that a second-order phase transition may take place in the U(4) vibron model in the large N limit. However, the boson number N is always finite when the vibron model is applied to real physical systems such as diatomic molecules and nuclear molecules. For example, the total boson number related to the number of the bound states in diatomic molecules ranges from tens to hundreds [39]. It is thus important to investigate how the characteristics of quantum phase transitions in the vibron model change with respect to the boson number N, especially in the case of N ranging from tens to hundreds more concerned in experiments.

One way to study the phase transitions in a system with the Hamiltonian of Eq. (3) at finite boson number N is to analyze its spectrum. To diagonalize the Hamiltonian of Eq. (3), we expand its eigenstates in terms of the wave function $|Nn_pL\rangle$ identified by the dynamical group chain $U(4) \supset U(3) \supset O(3)$ as

$$|NkL;\eta\rangle = \sum_{n_p} C_{n_p}^k(\eta) |Nn_pL\rangle, \tag{10}$$

where $C_{n_p}^k(\eta)$ is the expansion coefficient and k is an additional quantum number to distinguish the eigenstates with the same angular momentum L.

To show how the energy levels change as a function of the control parameter η and the total boson number N, we display the 25 low-lying energy levels with possible fixed angular momentum L for the system with $N = 10, 50$, and 100 in Fig. 2. It is seen from the figure that there are minima in the low-lying excitation energy and the locations of the minima for different energy levels are different in the case of $N = 10$, but with the increasing of the total boson number, all the minima of different energies get closer and closer to each other, and their locations converge to the critical point $\eta = 3/7$. This provides another signal that $\eta = 3/7$ is the critical point for the quantum phase transition to occur. One may also notice that some energy levels in different energy bands cross each other at the critical point, where the level density grows rather drastically and all the levels there tend to collapse to zero with the increase of boson number N. It appears that the physical system around the critical point may be more readily excited.

TABLE II. Some typical energy ratios and $B(E1)$ ratios with the E(3), U(3), and O(4) symmetries together with those at the critical point of the transition U(3)-O(4) [with $\eta = \frac{3}{7}$ in Eq. (3)] in the system with $N = 10, 50, 100$.

	E(3)	Critical point			U(3)	O(4)
		$N = 10$	$N = 50$	$N = 100$		
E_{2_1}/E_{1_1}	2.26	2.25	2.18	2.17	2	3
E_{3_1}/E_{1_1}	3.77	3.72	3.52	3.48	3	6
E_{0_2}/E_{1_1}	2.87	2.49	2.45	2.44	2	$2N$
$\frac{B(E1;2_1\to 1_1)}{B(E1;1_1\to 0_1)}$	1.59	1.53	1.69	1.72	$\frac{2(N-1)}{N}$	$\frac{6(N-1)(N+3)}{5N(N+2)}$
$\frac{B(E1;0_2\to 1_1)}{B(E1;1_1\to 0_1)}$	0.98	1.00	1.25	1.30	$\frac{2(N-1)}{N}$	0

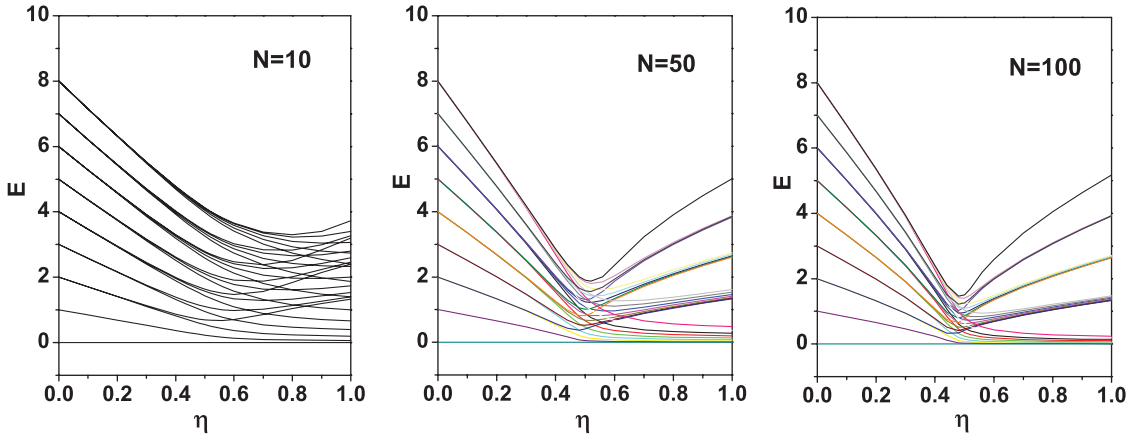

FIG. 2. (Color online) Variance of the 25 low-lying energy levels (in arbitrary unit) of the Hamiltonian in Eq. (3) with respect to the control parameter η for the system with $N = 10$ (left panel), 50 (middle panel), 100 (right panel).

We also give some typical energy ratios and $B(E1)$ ratios at the critical point $\eta = 3/7$ with different boson number together with those in both the U(3) and O(4) symmetry limits in Table II, where the $E1$ transition operator in vibron model is taken as $T(E1) = e_1(s^\dagger \tilde{p} + p^\dagger \tilde{s})^{(1)}$ with an effective charge e_1. The energies ratios, which is easy to be read out from Table I, and $B(E1)$ ratios in E(3) symmetry are also listed in Table II for comparison. Seen from Table II, all the energy ratios and $B(E1)$ ratios in the E(3) symmetry are well reproduced by those at the critical point; meanwhile, all of them lie in the between of the values in U(3) and O(4) symmetries. It should be noted that it is accidental that the ratios in E(3) symmetry seem to be closer to the case for $N = 10$ than those for larger N, because the true potential at the critical point is not the infinite well but $\sim x^4$ in the large N limit, and the similar feature exists in IBM [40]. Whatever, the E(3) symmetry can be taken as a good approximation to describe the property of the states at the critical point of U(3)-O(4) phase transition.

To identify the order of phase transition in the case of finite N, one can also study the behavior of quantal order parameter $\rho = \langle \hat{n}_p \rangle / N$, which is related with the classical order parameter x_e via the expression $\rho = \frac{1}{2}x_e^2$. According to the Hellmann-Feynman theorem, $\frac{\partial E_n}{\partial \eta} = \langle \frac{\partial H}{\partial \eta} \rangle_n$, we have $\frac{\partial E_0}{\partial \eta} = \frac{1}{\eta}(E_0 - n_p)$ and $\frac{\partial^2 E_0}{\partial \eta^2} = -\frac{1}{\eta}\frac{\partial n_p}{\partial \eta}$, where E_0 is the energy of the ground state and $n_p = \langle \hat{n}_p \rangle$ is the number of p bosons in the ground state. Following Refs. [7,16,17] for the U(6) IBM, the quantum order parameter ρ, and its derivative, $\rho' = \partial\rho/\partial\eta$, can be taken as signatures of the phase transition. The calculated results of ρ and its derivative, $\rho' = \partial\rho/\partial\eta$, as functions of η for the systems with $N = 10, 50, 100$, and ∞, respectively, are illustrated in Fig. 3, where the cases of $N = 10, 50, 100$ represent those concerned in experiments and the case of $N = \infty$ is obtained from the coherent state method. One can notice from the upper panel of Fig. 3 that the order parameter ρ increases gradually with the increasing of the control parameter η. The η corresponding to the maximum of $\rho' = \frac{\partial\rho}{\partial\eta}$ is denoted as $\eta_{\max}$. Figure 3 manifests evidently that the $\rho'|_{\eta=\eta_{\max}}$ is not very large and the $\eta_{\max}$ is quite large for the system with relatively small N (for example, $\eta_{\max} \approx 0.6$ in the case of $N = 10$). The $\rho'|_{\eta=\eta_{\max}}$ becomes larger and larger, whereas the $\eta_{\max}$ gets smaller and smaller with the increase of N and more and more approaches the critical point $\eta_c = 3/7$. In the large N limit, $\eta_{\max} = \eta_c$, and the order parameter keeps $\rho = 0$ in the left of η_c, whereas increases continuously with η in the right of η_c. Seen from the lower panel of Fig. 3, the peak of ρ' gets steeper and steeper at $\eta_{\max}$ with the increasing of N, and the value of ρ' at η_c is discontinuous in the large N limit. It indicates that $\frac{\partial^2 E_0}{\partial \eta^2}$ is discontinuous, whereas $\frac{\partial E_0}{\partial \eta}$ is continuous, in the large N limit, because the energy of ground state and the control parameter η are always continuous. Such a result confirms once more that the phase transition from U(3) symmetry to O(4) symmetry in the U(4) vibron model is a second-order quantum phase transition. The effect of the finite boson number N is only smoothing the transition process.

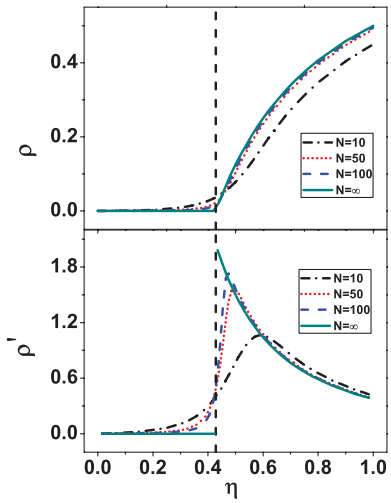

FIG. 3. (Color online) Calculated control parameter η dependence of the quantal order parameter ρ and its derivative ρ' of the system with the total bosons number $N = 10, 50, 100$, and ∞, respectively.

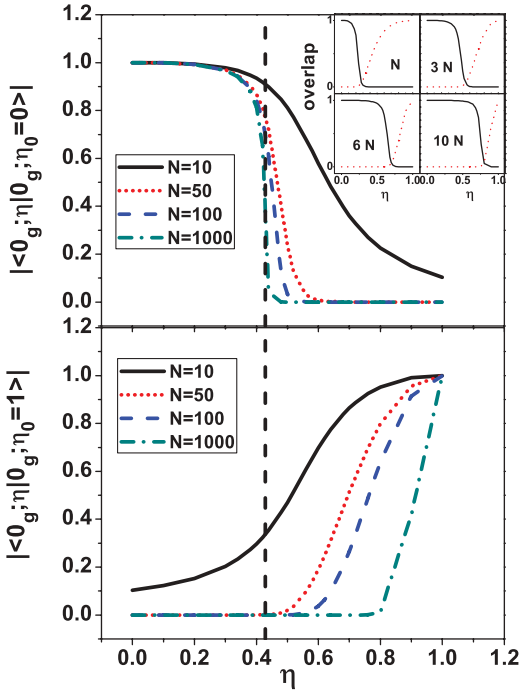

FIG. 4. (Color online) Calculated variation behavior of the overlap of the ground-state wave function with that in the cases of dynamical symmetries for the systems with total boson number $N = 10$, 50, 100, and 1000, respectively. The inset shows the overlaps at a fixed $N = 50$ with $f(N) = N, 3N, 6N$, and $10N$ in Eq. (3) as the function of η (the solid curve represents $|\langle 0_g;\eta|0_g;\eta=0\rangle|$, and the dashed line denotes $|\langle 0_g;\eta|0_g;\eta=1\rangle|$).

It has been shown previously that the overlap of the ground-state wave function with that in the dynamical symmetries may also serve as a signature of the phase transition [7,16,17], although it is unable to distinguish the first-order from the second-order transitions in the U(6) IBM [16,17]. We have calculated the overlap of the ground-state wave functions of the Hamiltonian in Eq. (3) $|\langle 0_g;\eta|0_g;\eta_0\rangle|$ with $\eta_0 = 0, 1$ of the systems with the total boson number $N = 10, 50, 100$, and 1000, respectively, where the case for $N = 1000$ is used to imitate the one for the large N limit. The obtained results are illustrated in Fig. 4. It shows that there is a sharp change in $|\langle 0_g;\eta|0_g;\eta=0\rangle|$ around the critical point $\eta = 3/7$ in the system with relatively large N. It indicates that the largest absolute value of the derivative of $|\langle 0_g;\eta|0_g;\eta=0\rangle|$ with respect to η occurs around the critical point $\eta_c = 3/7$ in the large N limit. As for $|\langle 0_g;\eta|0_g;\eta=1\rangle|$, it cannot be taken to locate the position of the critical point because a $1/N$ factor depresses the O(4) symmetry in Hamiltonian and this point can be seen more clearly in Fig. 1, where the ground states with different $\eta \in [0, \eta_c]$ are degenerate, and the degeneracy is broken as $\eta > \eta_c$, so that the values of $|\langle 0_g;\eta|0_g;\eta=1\rangle|$ gets nonzero only for those close to $|\eta = 1\rangle$. In the case of moderate number of bosons N, this situation is smoothed out. In addition, it can be clearly seen from the inset of Fig. 4 that the critical point η_c changes with different choices of the function $f(N) = aN$. The larger the value of a, the larger the value of the critical parameter η_c. $\eta_c \sim 0.2$ for $f(N) = N$,

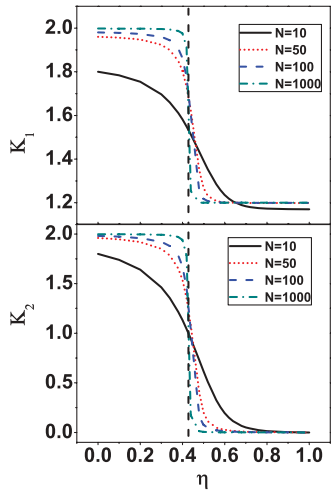

FIG. 5. (Color online) Calculated $B(E1)$ ratios $K_1 = \frac{B(E1;2_1\to 1_1)}{B(E1;1_1\to 0_1)}$ and $K_2 = \frac{B(E1;0_2\to 1_1)}{B(E1;1_1\to 0_1)}$ as a function of the control parameter η in the case of total boson number $N = 10$, 50, 100, 1000, respectively.

whereas $\eta_c \sim 0.7$ for $f(N) = 10N$, which agree with the analytical result in the large N limit (where $\eta_c = \frac{a}{4+a}$).

The $E1$ transition rate ratios $K_1 = \frac{B(E1;2_1\to 1_1)}{B(E1;1_1\to 0_1)}$ and $K_2 = \frac{B(E1;0_2\to 1_1)}{B(E1;1_1\to 0_1)}$ are also calculated, of which the values at the critical point for several cases of N are listed in Table II. It has been shown that the ratio of the cascade electromagnetic transition rates could be a signature of the nuclear shape phase transitions and distinguish their order [17]. The obtained results for the system with total boson number $N = 10$, 50, 100, 1000, respectively, are displayed in Fig. 5. It shows clearly that the ratios K_1 and K_2 change smoothly and monotonously against the increase of η in the case of small N, whereas there is a rather sharp change at the critical point when N is sufficiently large. One may also notice that the $B(E1)$ ratio remains relatively flat as the control parameter takes values smaller or larger than the critical one in the case of large total boson number (e.g., $N = 100, 1000$ in the figure), which is a peculiarity of a second-order phase transition, because the global behavior of $B(E1)$ ratio is very similar to the $B(E2)$ ratio in the second-order phase transition in the IBM [17]. Therefore, the $B(E1)$ ratio, as an observable quantity, may be taken as an effective order parameter [7] to identify the quantum phase transition in U(4) vibron model and its order. It may further help to identify experimental evidence for the phase transition. Moreover, the energies ratios E_{2_1}/E_{0_2} and E_{3_1}/E_{0_2} can also be taken as the effective order parameters to identify phase transitions and its order according to the analysis in Ref. [18], where the ratio E_{6_1}/E_{0_2} was implemented to distinguish the first-order from second-order phase transition in IBM. The calculated results in the present U(4) vibron model are shown in Fig. 6, where both ratios exhibit a rather flat behavior in the region out of the critical point, and a sharp change appears around the the critical point in the large N case that is quite similar to the behavior of E_{6_1}/E_{0_2} in the U(5)-O(6) phase transition in IBM [18]. It manifests that the energy ratios can work as well as the $B(E1)$ ratios and would be easier to measure in experiment.

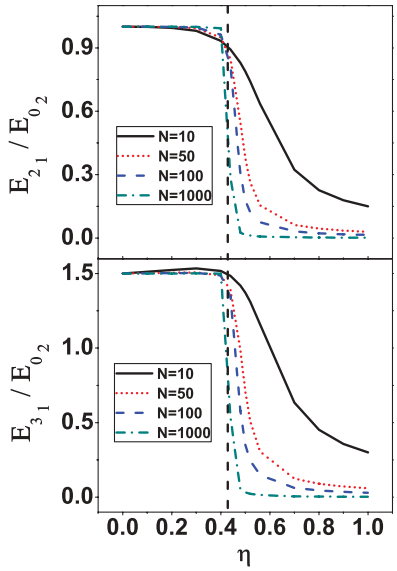

FIG. 6. (Color online) Calculated energiy ratios E_{2_1}/E_{0_2} and E_{3_1}/E_{0_2} as a function of the control parameter η in the case of total boson number $N = 10, 50, 100, 1000$, respectively.

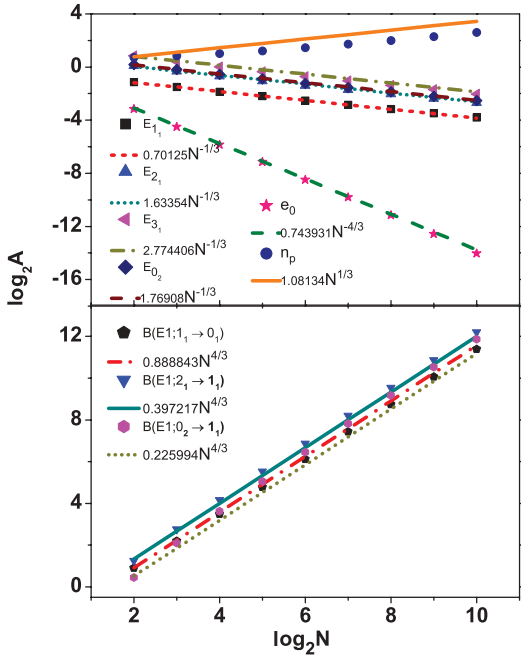

FIG. 7. (Color online) Calculated variation behavior of some typical energies E_{L_ξ}, $E1$ transition rates $B(E1)$, ground-state energy per boson e_0, and p-boson number n_p (denoted as A in general) at the critical point $\eta_c = \frac{3}{7}$ with respect to the boson number N (in $\log_2$-$\log_2$ scale. For $B(E1)$, the effective charge e_1 has been set to 1. For e_0 and n_p, what shown here are only their singular parts).

As shown in Refs. [9,11,12,41], there exists a scaling feature in the energy spectrum and other quantities at the critical point of a second-order phase transition. We then investigate such kind scaling characteristic of some quantities, including the ground-state energy per boson e_0, some typical excitation energies, and the p-boson number in the ground states in vibron model as well as that of some typical $B(E1)$ transition rates in numerical way. The obtained results are shown in Fig. 7. From the figure we can learn that all the excitation energies show a scaling property with $E \sim N^{-1/3}$ and all the $B(E1)$ transition rates display the other with $B(E1) \sim N^{4/3}$. Actually, a method of calculating the scaling exponents at the critical point in two-level boson systems has been introduced in Ref. [11,12], where a physical quantity A at the critical point is decomposed into a regular part and a singular part as $\mathrm{A}_N(\eta_c) = A_N^{\mathrm{reg}}(\eta_c) + A_N^{\mathrm{sing}}(\eta_c)$. The investigation in Ref. [11,12] shows that only the singular part $\mathrm{A}_N^{\mathrm{sing}}(\eta_c) \sim N^m$, where m is just the scaling exponent. Our present numerical results here indicate that the regular parts $\mathrm{A}_N^{\mathrm{reg}}(\eta_c)$ of all the excitation energies and $B(E1)$ transition rates equate definitely zero and in turn $\mathrm{A}_N(\eta_c) \sim N^m$. Such a scaling behavior is apparently consistent with that given in Ref. [11], where the finite-size scaling behaviors of some typical quantities at the critical point in two-level boson systems were studied by using the continuous unitary transformation (CUT) method. As for the ground-state energy per boson e_0, the regular part is not zero, therefore we need to take the CUT technique to work out the regular part and the singular part of e_0, respectively, and extract the scaling exponent of the singular part. We only show the concrete results because the CUT method in two-level bosons systems has been described in detail in Ref. [11], where the structure of Hamiltonian is very similar with that used here.

In the CUT approach, one can find that e_0 at η_c can be written as $e_0(\eta_c) = e_{0N}^{\mathrm{reg}}(\eta_c) + e_{0N}^{\mathrm{sing}}(\eta_c)$, where $e_{0N}^{\mathrm{reg}}(\eta_c) = -\frac{3}{2N}(1-\eta_c) - \frac{1}{N^2}\eta_c$, and $e_{0N}^{\mathrm{sing}}(\eta_c) = \frac{1}{N}\frac{3\Xi(\eta_c)^{1/2}}{2} + \frac{1}{N^2}B_1 + \frac{1}{N^3}B_2 + O(1/N^4)$ with $\Xi(\eta_c) = (1-\eta_c)[\frac{7}{3}(1-\eta_c) - \frac{4}{3}]$. In the vicinity of the critical point, the divergent terms have a leading order contribution that is proportional to $\Xi(\eta_c)^{-1}$ for B_1 and to $\Xi(\eta_c)^{-5/2}$ for B_2, then the singular part can be written as $e_{0N}^{\mathrm{sing}}(\eta_c) \approx \frac{\Xi(\eta_c)^{\xi_\Phi}}{N^{n_\Phi}}\Pi_\Phi[N\Xi(\eta_c)^{3/2}]$ with $\Pi_\Phi(y) \sim y^{-2\xi_\Phi/3}$ according to the analysis in Ref. [11]. It is easy to gain $e_{0N}^{\mathrm{sing}}(\eta_c) \sim N^m$, where the scaling exponent $m = -(n_\Phi + 2\xi_\Phi/3)$. Consequently, $e_{0N}^{\mathrm{sing}}(\eta_c) \sim N^{-4/3}$ because one has $n_\Phi = 1$ and $\xi_\Phi = 1/2$ for e_0, which is consistent with the numerical results shown in the upper panel of Fig. 7, where the scaling behaviors of e_0 and n_p are in fact only their singular part, respectively. One can also find the quantal order parameter $\rho(\eta_c)$ with $\rho_N^{\mathrm{reg}}(\eta_c) = -\frac{3}{2} + \frac{1}{N}$ and $\rho_N^{\mathrm{sing}}(\eta_c) \sim N^{-2/3}$ as well as its derivative $\rho'(\eta_c) = \rho'^{\mathrm{sing}}_N(\eta_c) \sim N^0$ according to the Hellmann-Feynman theorem. The result of $\rho_N^{\mathrm{sing}}(\eta_c) \sim N^{-2/3}$ is consistent with that of $n_p \sim N^{1/3}$ shown in Fig. 7 because $\rho = \frac{n_p}{N}$, and $\rho'(\eta_c) \sim N^0$ can be confirmed by the fact that $\rho'(\eta)$'s with different N cross with each other at almost one point at η_c shown in the lower panel of Fig. 3. By the way, it may be remarkable that one should pay more attention to the quantities A with the singular part $A_N^{\mathrm{reg}}(\eta_c) = 0$ when discussing the scaling behavior in experiment, because it is difficult to separate the $\mathrm{A}_N^{\mathrm{reg}}(\eta_c)$ and $\mathrm{A}_N^{\mathrm{sing}}(\eta_c)$ from each other in measurement.

It has been well known that once two quantities have the same scaling exponent, the ratio between them at the critical point must approach a constant independent of the total bosons number N. One can infer then that the E(3) symmetry defined

in the classical limit should work well even in the case of small N. Therefore, the results listed in Table II are just a good manifestation of the scaling behavior of the quantities at the critical point.

IV. A POSSIBLE EMPIRICAL EXAMPLE IN THE E(3) SYMMETRY

The U(4) vibron model was originally developed to describe the ro-vibration spectra of diatomic molecules, where most diatomic molecules are quasirigid and deviate little from the O(4) limit [39]. From the above analysis, we can learn that the potential energy surface around the critical point is rather flat, and the systems near the critical point may be excited more easily. It appears that the U(3)-O(4) transition may be used to describe the so-called floppy molecules [42]. The U(4) vibron model may also be extended easily to the case of polyatomic molecules [20], where there are more abundant data concerning phase transitions, such as the triatomic molecules corresponding to U(4)⊗U(4) model that exhibit phase transitions from linear to bent shapes [21]. The analysis in this article is general, because U(4) is the basic building block of many other extended models. Due to the similar structure of the spectra between U(4) and U(3) models [43,44], the results in this article may help to understand the dynamical behavior of U(2)-O(3) transitions in the U(3) model with a finite boson number N. Actually, a detailed account of the shape phase transition in U(3) model has been given in Ref. [45].

Another application of the U(4) model is the description of nuclear molecules [46–48]. A nuclear vibron model for nuclear molecules consisting of two clusters holds a $G_{C1} \otimes G_{C2} \otimes U_R(4)$ dynamical symmetry, where the internal structure of the ith cluster is described by G_{Ci} which may be, for example, the U(6) IBM or SU(3) shell model, and the relative motion between the clusters is described by the $U_R(4)$ vibron model. Sometimes only the U(4) vibron model itself is sufficient to describe the rotational and vibrational excitations in nuclear molecules, where the internal structure of each cluster does not play an essential role in the low-lying levels, such as the narrow resonances in the $^{12}C + ^{12}C$ system [28,29]. Initially, the O(4) limit of U(4) vibron model was proposed to describe the resonant energies of $^{12}C + ^{12}C$ system [28], whereas the analysis in Ref. [29] indicates that the U(3) limit may be preferred when fitting the resonances. To compare directly the experimental data with U(4) vibron model, we list some ratios of the low-lying resonant energies of the $^{12}C + ^{12}C$ system as well as the corresponding results with U(3), O(4), and E(3) symmetries in Table III. One can find in Table III that E(3) symmetry shows a better coincidence with the experiment data than U(3) and O(4) symmetries. It provides a clue that the bottom of the potential in the $^{12}C + ^{12}C$ system is rather flat. An exception should be noted is that the ratio E_{0_2}/E_{2_1} is closed to zero which means E_{0_2} is approximatively degenerate with the ground-state energy E_{0_1}, then E_{0_3}/E_{2_1} shown in the parentheses of Table III can be implemented to compare with the theoretical results instead of E_{0_2}/E_{2_1}. As for the higher resonant energies, there is a systematic deviation between experiments and theory because the Hamiltonian used here is rather simple, and more interaction terms in vibron model as well as the effects of the internal structure of the subcluster should be considered to completely reproduce the resonant energies of $^{12}C + ^{12}C$ system [30]. These results show globally that E(3) symmetry can be taken as a better starting point than U(3) symmetry limit to fit the resonant energies of $^{12}C + ^{12}C$. One may infer then that $^{12}C + ^{12}C$ system is an empirical example of the one with E(3) symmetry approximately.

TABLE III. The experimental energies ratios of $^{12}C + ^{12}C$ system and the corresponding energies ratios with E(3), U(3), and O(4) symmetry (the experiment data are taken from Ref. [48]).

	Expt.	E(3)	U(3)	O(4)
E_{4_1}/E_{2_1}	2.22	2.44	2	$\frac{10}{3}$
E_{6_1}/E_{2_1}	5.72	4.31	3	7
E_{0_2}/E_{2_1}	0.31(1.86)	1.27	1	$\frac{2N}{3}$
E_{2_2}/E_{2_1}	2.50	3.12	2	$\frac{2N}{3}+1$
E_{4_2}/E_{2_1}	4.48	5.44	3	$\frac{2N}{3}+\frac{10}{3}$
E_{6_2}/E_{2_1}	7.55	8.22	4	$\frac{2N}{3}+7$

V. SUMMARY

In summary, we have analyzed the U(3)-O(4) quantum phase transition in the U(4) vibron model for both the case of large boson number limit and the situation of finite boson number N. We show that the second-order phase transition still persist for the boson number N ranging from tens to hundreds in the U(4) vibron model, and the critical point with a relative flat potential in large N limit can be approximately described by the E(3) symmetry even for a more realistic bosons number. Two ratios of $E1$ transition rates and two energies ratios can be taken as effective order parameters to identify the phase transition for both the large N limit and the finite N case. Furthermore, the effect of a finite boson number is shown to merely shift the location of the singular point $\eta_{\max}$ away from the critical point η_c, and smooth out the characteristic of the phase transition in large N limit but maintain the scaling properties well for the energies and E1 transition rates that guarantees E(3) symmetry to work independent of the bosons number N. It is easy to extend above conclusion to other representation symmetries because the finite-size scaling behavior exists universally in the second-order phase transitions [11]. As for the first-order phase transition, the representation symmetry seems to work well too [35], but there is not a simple scaling behaviors for quantities at the critical point, which is still an open question [9].

On the experimental side, there has been a preliminary evidence of the E(3) symmetry. However more investigations are needed to eventually confirm or disprove the theoretical predictions. Related work is under progress.

ACKNOWLEDGMENTS

This work was supported by the National Natural Science Foundation of China under contract nos. 10425521 and 10675007, the Major State Basic Research Development Program under contract no. G2007CB815000, the Key Grant Project of Chinese Ministry of Education (CMOE) under contact no. 305001, and the Research Fund for the Doctoral Program of Higher Education of China under grant no. 20040001010.

[1] J. N. Ginocchio and M. W. Kirson, Phys. Rev. Lett. **44**, 1744 (1980).
[2] A. E. L. Dieperink, O. Scholten, and F. Iachello, Phys. Rev. Lett. **44**, 1747 (1980).
[3] D. H. Feng, R. Gilmore, and S. R. Deans, Phys. Rev. C **23**, 1254 (1981).
[4] P. Van Isacker and J. Q. Chen, Phys. Rev. C **24**, 684 (1981).
[5] F. Iachello and A. Arima, *The Interacting Boson Model* (Cambridge University, Cambridge, UK, 1987).
[6] J. Jolie, P. Cejnar, R. F. Casten, S. Heinze, A. Linnemann, and V. Werner, Phys. Rev. Lett. **89**, 182502 (2002).
[7] F. Iachello and N. V. Zamfir, Phys. Rev. Lett. **92**, 212501 (2004).
[8] D. J. Rowe, Phys. Rev. Lett. **93**, 122502 (2004).
[9] D. J. Rowe, P. S. Turner, and G. Rosensteel, Phys. Rev. Lett. **93**, 232502 (2004).
[10] P. Cejnar, S. Heinze, and J. Dobeš, Phys. Rev. C **71**, 011304(R) (2005).
[11] S. Dusuel, J. Vidal, J. M. Arias, J. Dukelsky, and J. E. García-Ramos, Phys. Rev. C **72**, 064332 (2005).
[12] J. M. Arias, J. Dukelsky, J. E. García-Ramos, and J. Vidal, Phys. Rev. C **75**, 014301 (2007).
[13] D. D. Warner and R. F. Casten, Phys. Rev. C **28**, 1798 (1983).
[14] A. Leviatan, Phys. Rev. Lett. **77**, 818 (1996); **98**, 242502 (2007); A. Leviatan and P. Van Isacker, Phys. Rev. Lett. **89**, 222501 (2002).
[15] Y. X. Liu, L. Z. Mu, and H. Wei, Phys. Lett. **B633**, 49 (2006).
[16] F. Pan, Y. Zhang, and J. P. Draayer J. Phys. G **31**, 1039 (2005).
[17] Y. Zhang, Z. F. Hou, and Y. X. Liu, Phys. Rev. C **76**, 011305(R) (2007).
[18] D. Bonatsos, E. A. McCutchan, R. F. Casten, and R. J. Casperson, Phys. Rev. Lett. **100**, 142501 (2008).
[19] For recent review, see, for example, R. F. Casten and E. A. McCutchan, J. Phys. G **34**, R285 (2007).
[20] F. Iachello and R. D. Levine, *Algebraic Theory of Molecules* (Oxford University, Oxford, UK, 1995).
[21] S. Kuyucak, Chem. Phys. Lett. **301**, 435 (1999).
[22] F. Pérez-Bernal, L. F. Santos, P. H. Vaccaro, and F. Iachello, Chem. Phys. Lett. **414**, 398 (2005).
[23] H. Yépez-Martínez, J. Cseh, and P. O. Hess, Phys. Rev. C **74**, 024319 (2006).
[24] F. Iachello and R. D. Levine, J. Chem. Phys. **77**, 3046 (1982).
[25] S. Kuyucak and M. K. Roberts, Chem. Phys. Lett. **238**, 371 (1995).
[26] S. Kuyucak and M. K. Roberts, Phys. Rev. A **57**, 3381 (1998).
[27] F. Iachello, Phys. Rev. C **23**, 2778(R) (1981).
[28] K. A. Erb and D. A. Bromley, Phys. Rev. C **23**, 2781 (1981).
[29] J. Cseh, Phys. Rev. C **31**, 692 (1985).
[30] J. Cseh, G. Lévai, and W. Scheid, Phys. Rev. C **48**, 1724 (1993).
[31] F. Iachello, N. C. Mukhopadhyay, and L. Zhang, Phys. Rev. D **44**, 898 (1991).
[32] F. Pan, Y. Zhang, and J. P. Draayer, Eur. Phys. J. A **A28**, 313 (2006).
[33] O. S. Van Roosmalen and A. E. L. Dieperink, Ann. Phys. (NY) **139**, 198 (1982).
[34] F. Iachello, Phys. Rev. Lett. **85**, 3580 (2000).
[35] F. Iachello, Phys. Rev. Lett. **87**, 052502 (2001).
[36] R. F. Casten and N. V. Zamfir, Phys. Rev. Lett. **85**, 3584 (2000); A. Frank, C. E. Alonso, and J. M. Arias, Phys. Rev. C **65**, 014301 (2001); D. L. Zhang and Y. X. Liu, Phys. Rev. C **65**, 057301 (2002); R. M. Clark *et al*., Phys. Rev. C **69**, 064322 (2004).
[37] R. F. Casten and N. V. Zamfir, Phys. Rev. Lett. **87**, 052503 (2001); R. Krucken *et al*., Phys. Rev. Lett. **88**, 232501 (2002); D. L. Zhang and Y. X. Liu, Chin. Phys. Lett. **20**, 1028 (2003); D. Tonev *et al*., Phys. Rev. C **69**, 034334 (2004); A. Dewald *et al*., Eur. Phys. J. A **20**, 173 (2004).
[38] P. Cejnar and F. Iachello, J. Phys. A **40**, 581 (2007).
[39] F. Pan, X. Zhang, and J. P. Draayer, Phys. Lett. **A316**, 84 (2003).
[40] J. M. Arias, C. E. Alonso, A. Vitturi, J. E. García-Ramos, J. Dukelsky, and A. Frank, Phys. Rev. C **68**, 041302(R) (2003).
[41] S. Dusuel, J. Vidal, J. M. Arias, J. Dukelsky, and J. E. García-Ramos, Phys. Rev. C **72**, 011301(R) (2005).
[42] F. Iachello and S. Oss, Eur. Phys. J. D **19**, 307 (2002).
[43] F. Iachello, F. Pérez-Bernal, and P. H. Vaccaro, Chem. Phys. Lett. **375**, 309 (2003).
[44] F. Pan, Y. Zhang, S. Jin, J. P. Drayyer, M. L. Ge, and J. L. Birman, Phys. Lett. **A341**, 291 (2005).
[45] F. Pérez-Bernal and F. Iachello, Phys. Rev. A **77**, 032115 (2008).
[46] F. Iachello, Nucl. Phys. **A421**, 97c (1984).
[47] H. J. Daley and F. Iachello, Ann. Phys. (NY) **167**, 73 (1986).
[48] H. Yépez-Martínez, P. O. Hess, and S. Misicu, Phys. Rev. C **68**, 014314 (2003).